RSC Advances

ROYAL SOCIETY OF CHEMISTRY

www.rsc.org/advances

Cite this: DOI: 10.1039/c0xx00000x

www.rsc.org/xxxxxx

ARTICLE TYPE

Chaos to order: an eco-friendly way to synthesize graphene quantum dots

Ying Huang, Chiyao Bai, Kecheng Cao, Yin Tian, Yue Luo, Chuanqin Xia, Songdong Ding, Yongdong Jin, Lijian Ma* and Shoujian Li*

Received (in XXX, XXX) Xth XXXXXXXXX 20XX, Accepted Xth XXXXXXXXX 20XX
DOI: 10.1039/b000000x

We have developed a rapid, simple and pollution-free method to synthesize highly ordered graphene quantum dots (GQDs) which adopts cheap and readily available activated carbon and environmental friendly hydrogen peroxide as raw materials through simple microwave and hydrothermal treatment, and the fine products are obtained as size uniform particles. The proposed strategy realizes the tough transformation from amorphous carbon to highly ordered GQDs for the first time which completely avoids using concentrated sulphuric acid, concentrated nitric acid and other caustic reagent, and the purification procedure is relatively easy to achieve. Furthermore, the as-prepared products possess low toxicity, high biological compatibility and good fluorescence property, which exhibit excellent properties in bio-labelling application.

1. Introduction

Graphene, a two-dimensional (2D) monolayer graphite consisting of sp^2-hybridized carbon atoms, was first obtained by K. S. Novoselov and A. K. Geim via mechanical exfoliation in 2004[1]. Its extremely high mechanical strength, chemical stability, good electrical conductivity at room temperature than any other known materials and long-range π-conjugation that yields a half-integer quantum hall effect and an ambipolar electric field effect make it a superstar in material realm[2].

In comparison with conventional two-dimensional (2D) graphene, zero-dimensional (0D) graphene quantum dots (GQDs) are clusters stacked from several layers of graphene with nanometer diameter, which usually contain some oxygen-rich functional groups, such as hydroxy, carboxyl , epoxy groups on their edges[3]. Furthermore, GQDs with high quantum yield also contain some nitrogen-containing functional groups after passivating treatment [4, 5]. As a newly coming carbonaceous nanomaterial derived from graphene, GQDs not only possess quantum hall effect at room temperature, but also show characteristic quantum confinement effect and strong photoluminescence (PL) character. Compared with the traditional semiconductor quantum dots which are synthesized from toxic metal compound such as CdS[6], GQDs' outstanding biological compatibility, low toxicity and good dispersibility in many kinds of solvents make it a promising material in bioimaging, photovoltaic and light emitting fields[3].

Up to now, the reported methods to synthesize GQDs mainly contain nanolithography technique[7], electrochemical scissoring[8], ultrasonic shearing[9], hydrothermal and solvothermal cutting of graphene sheets (GSs) [10, 11], nanotomy assisted exfoliation [12], precursor pyrolysis [13] and stepwise organic synthesis etc. [14]. Almost all the methods need to utilize some sophisticated, expensive equipments and/or require harsh conditions. Moreover, the separation and purification processes are extremely cumbersome and the purity of product is not satisfactory. It also should be noted that the precursors used in most of these methods are highly ordered graphite as well as its derivatives. Not only the price of raw materials is relatively expensive, but also the modified Hummers method needs to be employed to obtain graphite oxide firstly before the preparation of GQDs[15,16,17]. As is known to all, during the preparation of graphite oxide via Hummers method, some harsh and environmental unfriendly chemicals, such as fuming sulfuric acid, concentrated nitric acid, and potassium permanganate are used unavoidably. Besides, washing the product needs large volume of water and the proceedings inevitably introduce secondary pollution to the product. All these deficiencies have become bottlenecks of the commercial production of GQDs.

In order to solve the problems mentioned above, we innovatively exploited a green way to synthesize GQDs which adopted cheap and readily available activated carbon and environmentally friendly hydrogen peroxide instead of other

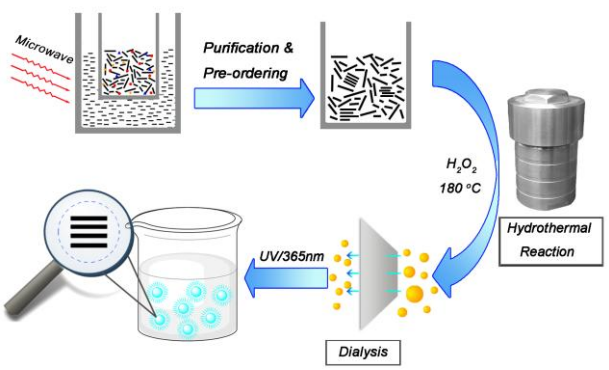

Scheme 1 Graphical representation of the synthesis of GQDs

tough to degrade reagent as raw materials through microwave assisted preliminary ordering and purification and simple hydrothermal reaction, and the fine products (GQDs-SH) were obtained as size uniform particles after dialysis. The overall synthetic procedure is illustrated in scheme 1. GQDs-SH exhibits good stability and dispersity and excellent solubility (stored for 6 months without aggregation). The particle size distributions are uniform and 85.9% are located in 4.5-10nm intervals and the quantum yield is as high as 9.8% (without using any passivant). The as-prepared GQDs-SH exhibits good chemical stability and low toxicity, excellent solubility and biocompatibility.

2. Results and discussions

2.1 XRD and PL characterization

The structure of GQDs-SH is further studied using X-ray diffraction (XRD) as shown in Fig. 1. The diffraction peak at 2θ = 26.56 ° is attributable to the rather limited ordering (only a few layers) graphite structure in microwave treated activated carbon[18]. Compared with the original activated carbon, the peak at 2θ = 26.56 ° becomes more sharpen after being treated in microwave oven, which indicates that microwave irradiation may lead to a pre-ordering process of the activated carbon as well as the removing of organic impurities in the raw materials. Microwave irradiation has been accepted as a useful method for syntheses of organic and inorganic compounds due to its distinct advantages such as uniform, rapid and volumetric heating, energy efficient[19,20], which result in a quick increase of temperature in the system and more efficient removal of some small molecules and functional groups in the activated carbon. After the irradiation, the activated carbon tends to become a more compact and orderly structure, which is proved by XRD spectra. As shown in Fig. 1, the (001) and (002) diffraction peaks of GQDs-SH are corresponding to graphite oxide and graphite's characteristic peaks[21], respectively.

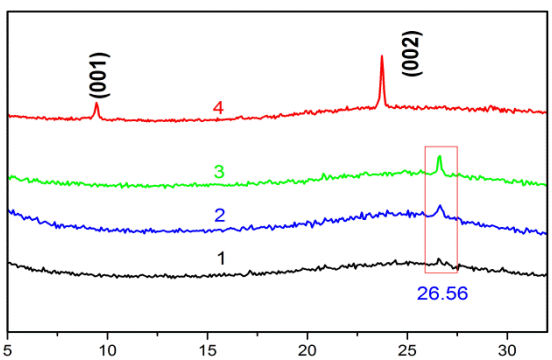

Fig. 1 XRD spectra of GQDs-SH (line 4), activated carbon under six minutes microwave treatment (line 3), under three minutes microwave treatment (line 2), raw activated carbon (line 1)

The (002) peak indicates that GQDs-SH contains graphite-like structure[22] and the graphite oxide (001) peak denotes that the product contains some functional groups such as –OH, –COOH, epoxy/ether, originated from the oxidization of H_2O_2 and O_2 which rooted in the decomposition of H_2O_2. Because of these groups the interlayer spacing of GQDs-SH becomes larger than graphite so the 2θ angle is smaller than 26.56 °. These functional groups are also proved by Fourier transform infrared spectra (FT-IR) and X-ray photoelectron spectroscopy (XPS).

A detailed PL study was carried out by using different excitation wavelengths to explore the optical properties of GQDs-SH. The PL spectra with excitation wavelengths from 280 to 440 nm are shown in Fig. 2. From the figure we can find that the emission intensity increases firstly with the increase of excitation wavelength, and the emission intensity reach a climax when excitation wavelength is 320nm, then the emission intensity decreases with the increase of excitation wavelength. Generally speaking, the PL spectra of most luminescent carbon nanoparticles are dependent on excitation wavelength.

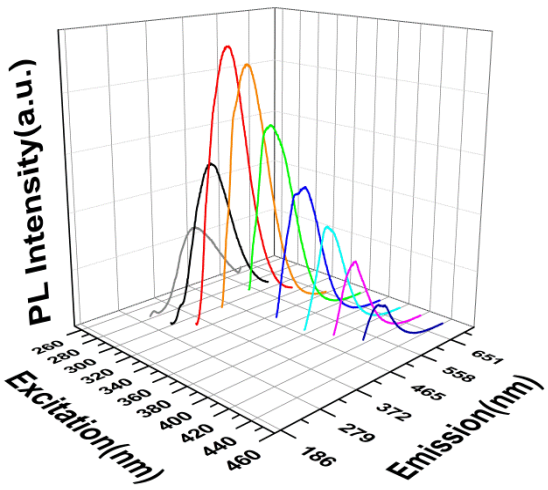

Fig. 2 PL emission spectra of GQDs-SH

However, GQDs-SH shows an excitation-independent PL feature. When excitation wavelength changes from 280 to 360 nm, the PL spectra are almost invariable and show a strong peak at ca. 420 nm (see Fig. S1, ESI†), which indicates that both the size and the surface state of those sp^2 clusters should be uniform[23]. The UV-vis absorption spectrum of GQDs-SH (see Fig. S2, ESI†) shows an absorption band at ca. 286 nm, which reveals a blue-shift of ca. 36 nm with respect to that of the reported GQDs[24]. It has been reported that due to the localization of electron-hole pairs, the isolated sp^2 hybridized clusters with size of ca. 3 nm within the carbon oxygen matrix could yield band gaps consistent with blue emission[25], which, along with the previous observation of PL from nanosized graphene oxide[26], indicates that the oxygen-rich groups make a significant contribution to the observation of blue shift in the PL emission besides the size and surface effects[27].

2.2 XPS analysis

Fig. 3(a) and (b) show the XPS analysis of C1s and O1s of GQDs-SH, respectively. The XPS C1s spectra of GQDs-SH show three characteristics peaks at 283.2, 284.9, and 286.7 eV. The binding energy (BE) of 283.2 eV is in close agreement with the values obtained by conventional XPS[28]. The 284.9 eV peak

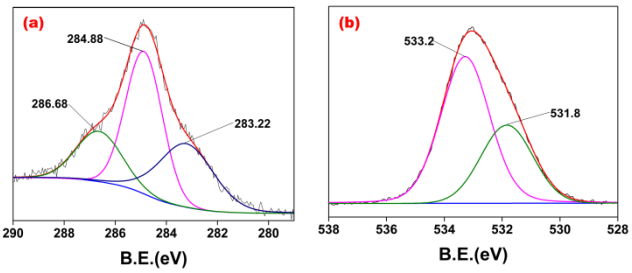

Fig. 3 XPS spectra of GQDs-SH: (a) C1s peaks and (b) O1s peaks.

reveals that the products exhibit graphite-like sp^2 hybrid carbon which is in good accordance with the XRD results. Furthermore, the 286.7 eV –C–O BE is another proof of C–OH stretching vibration in FTIR. The O1s peak at 531.8 eV in Fig. 3(b) is assigned to contributions from C=O and O=C–OH groups, referring to the peaks of C1s, and the peak at 533.2 eV is assigned to C–OH groups. In addition, area of the peak at 533.2 eV is larger in Fig. 3(b), which indicates the content of hydroxyl is more than that of carboxyl.

2.3 TEM images and FT-IR spectra

The transmission electron microscope (TEM) images of GQDs-SH are showed in Fig. 4. Through the TEM images we can reach a conclusion that GQDs-SH synthesized by this green strategy possesses well dispersibility and stability which also can be further proved by TEM images measured 6 months later, where there are no obvious agglomerations even after six-month storage (see Fig. S3, ESI†). The size distribution histogram (see Fig. 4(c)) indicates that the particle sizes of GQDs-SH are mostly (85.9%, calculated by statistics) concentrated in the range 4.5–10 nm, suggesting that GQDs-SH is uniform in dimension and the average diameter is 7 nm (calculated), similar to the reported[29].

Since the reaction is conducted under hydrothermal conditions at 180 ℃ in a hydrothermal tank and the H_2O_2 is easy to decompose into H_2O and O_2 under high temperature and pressure conditions, the as-synthesized GQDs-SH consequently contains some oxygen-containing functional groups, just as the exhibition

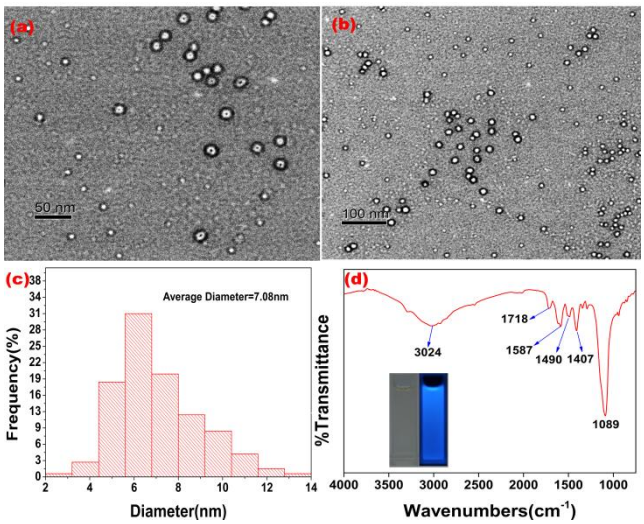

Fig. 4 TEM images scale bar: (a) 50 nm, (b) 100 nm. (c) Size distribution of GQDs-SH. (d) FT-IR spectra. Insert: photographs of aqueous solutions of the GQDs-SH (left) under naked eye and (right) under UV lights (365nm).

of traditional method. As is can be seen from the FT-IR spectra in Fig. 4(d), GQDs-SH displays a stretching vibration of O–H at 3024 cm^{-1} and a characteristic peak of C=O at 1718 cm^{-1}, while the peak intensity is really weak, indicating the low carbonyl. The peaks at 1587 cm^{-1}, 1490 cm^{-1} and 1407 cm^{-1} demonstrate that the product possesses benzene ring structure which in accordance with the XRD results. Moreover, a strong C–OH stretching vibration peak is appeared at 1089 cm^{-1}, indicating GQDs-SH is rich in hydroxyl which could be further explored to apply in fields of biolabeling, fluorescent detecting, etc.

2.4 AFM characterization and cytotoxicity

The AFM image and the height profile of GQDs-SH are shown in Fig. 5. The topographic heights of the products are mainly between 2.5–5 nm according to the image. Consequently, it can be concluded that most of the GQDs-SH particles are consisted of less than 5 layers graphene, although some heights in the profile are more than 10 nm, which is probably come from the preparing process of the AFM testing samples in which the GQDs-SH solution is drip onto mica plate repeatedly and the overlap of GQDs-SH could be inevitable.

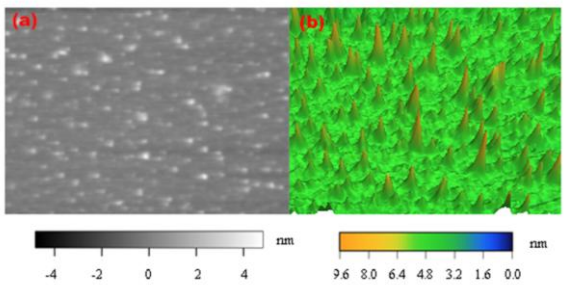

Fig. 5 (a) AFM images of the GQDs-SH on Si substrate, and (b) the height profile of the GQDs-SH.

As the method proposed in this article completely avoids the use of toxic raw materials and reagents and the quantum yield is satisfactory under the circumstance of no passivating agent, we investigate their biocompatibility and bio-labelling application using Hela cells. After 24 h incubation, the survival rate is higher than 80 % even if the concentration of GQDs-SH increases up to 400μg/mL (see Fig. 6(a)), which indicates the fairly low toxicity of GQDs-SH. The excellent biocompatibility demonstrated by the as-prepared GQDs-SH could be attributed to the completely green preparation procedure which adapts non-toxic H_2O_2 and active carbon as raw materials. Next, cell imaging was performed on an inverted florescence micro-scope after incubating Hela cells with GQDs-SH (100μg/mL) for 2 h. The bright-field image in Fig. 6(b) shows that the treated cells retain their original fusiform morphology, confirming the low-toxicity of the GQDs-SH. Fluorescent image in Fig. 6(c) and overlay image in Fig. 6(d) both show that Hela cells labeled by GQDs-SH shine strong blue ray under the UV irradiation, which further indicates that our materials could serve as a promising agent for optical imaging.

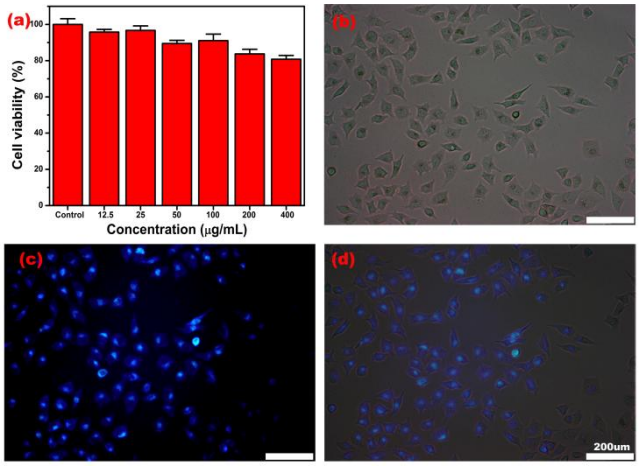

Fig. 6 Cellular toxicity and cellular imaging of GQDs. (a) Effect of GQDs-SH on Hela cells viability. (b) Bright field (c) Fluorescent field (d) Overlay images of labelled Hela cells.

3. Conclusions

In summary, GQDs-SH with strong blue fluorescent has been prepared via simple microwave treatment and hydrothermal reaction from activated carbon and a tough transformation from amorphous carbon to highly ordered GQDs was achieved for the first time in this course. This approach is energy, material, and labour efficient. Moreover, it satisfies with the several principles of green chemistry. Fluorescence quantum yield of the product is as high as 9.8% without the usage of any passivating agent. The resulting GQDs-SH is well-dispersed and shows an excitation-independent PL feature. This novel nanomaterial possesses the ability of easy to penetrate live cells, remarkable PL property, nontoxicity to cells and holds a great potential for biomedical applications.

4. Experimental Section

4.1 Microwave irradiation procedures

Accurately weighted amount 0.6g activated carbon (AC) was put into a smaller quartz crucible and then placed the crucible into a bigger one, the interspaces between the two crucibles were filled with powder graphite. Then they were put into a modified domestic microwave oven (adjusted to 800 W) heated for six minutes under atmosphere condition. After the heating procedure, let the sample cool down to room temperature under atmosphere.

4.2 Hydrothermal procedures

The microwave purified AC was cooled down to room temperature naturally, then the AC were mixed with 15mL H_2O_2 (30%) and transferred to a 25mL Teflon®-lined stainless steel autoclave which was then sealed and heated in an oven equipped with a thermostat or an automatic temperature control unit. The reaction temperature was raised to 180℃ from room temperature in 90 minutes and maintained thereat for 15 h. After cooling down, the colloidal solution was obtained and then dialyzed in a dialysis bag (retained molecular weight 8000-14000 Da) overnight and diluted with distilled water to 25mL.

4.3 Dialysis treatment

Dialysis bag (6-8cm) was boiled for 5 minutes and then dipped into 50% ethanol for half an hour. After that, the bag was washed with EDTA and distilled water in sequence. Then seal the raw product into the dialysis bag and dialyzed in water for 24 h to obtain size uniform particles.

4.4 Quantum Yields (QYs) calculation

Quinine sulfate in 0.10 M H_2SO_4 solution was used as standards. The QYs of GQDs (in water) were computed according to the formula underlying.

$$\Phi = \Phi_R \times \frac{I}{I_R} \times \frac{A_R}{A} \times \frac{\eta^2}{\eta_R^2}$$

Where Φ is the quantum yield, I is the measured integrated emission intensity, η is the refractive index of the solvent, and A is the optical density. The subscript *R* refers to standard index of the quinine sulfate (data are listed in Table S1).

4.5 Cell cultivation and cytotoxicity test

Hela cells were cultured with Dulbecco's Modified Eagle Medium (DMEM, high glucose) medium supplemented with 10% fetal bovine serum seeded in a flask under a humidified environment at 37°C with 5% of the CO_2 concentration. In vitro cytotoxicity was tested through performing CCK-8 assay on the cells. Hela cells were incubated in 96-well culture plates at a density of 2×10^3 cells per cell in 100μl fresh culture medium and cultivate for 24 h. Then, use PBS to wash the cells, and replace the medium with a fresh medium which contain a planed amount of testing materials. 24 h later, the cells were washed with PBS and cultivated in DMEM which contain 10% CCK-8 for 2 h. The absorbance of each well was measured at 450nm with a plate reader.

The financial supports from the National Natural Science Foundation of China (Grants 21171122, 21271132, 91126016, J1210004, J1103315 and J1310008), Chinese Academy of Sciences (Grant KJCX2-YW-N50-3) and the International Collaboration Project of Science and Technology Program of Sichuan Province, China (Grant 2010HH0008) are gratefully acknowledged.

Notes and references

[a] *Address, Address, Town, Country. Fax: XX XXXX XXXX; Tel: XX XXXX XXXX; E-mail: xxxx@aaa.bbb.ccc*
[b] *Address, Address, Town, Country. Fax: XX XXXX XXXX; Tel: XX XXXX XXXX; E-mail: xxxx@aaa.bbb.ccc*

† Electronic Supplementary Information (ESI) available: [details of any supplementary information available should be included here]. See DOI: 10.1039/b000000x/

‡ Footnotes should appear here. These might include comments relevant to but not central to the matter under discussion, limited experimental and spectral data, and crystallographic data.

1 K. S. Novoselov, A. K. Geim, S. V. Morozov, D. Jiang, Y. Zhang, S. V. Dubonos, I. V. Grigorieva and A. A. Firsov, *Science*, 2004, **306**, 666669.
2 Q. Tang, Z. Zhou and Z. F. Chen, *Nanoscale*, 2013, **5** , 4541.
3 J. H. Shen, Y. H. Zhu, X. L. Yang and C. Z. Li, *Chem. Commun.*, 2012, **48**, 3687.
4 Y. Q. Dong, R. X. Wang, G. L. Li, C. Q. Chen, Y. W. Chi, and G. N. Chen, *Anal. Chem.* 2012, **84**, 6220
5 L. L. Li, J. Ji, R. Fei, C. Z. Wang, Q. Lu, J. R. Zhang, L. P Jiang, and J. Jie, *Adv. Funct. Mater.* 2012, **22**, 2972
6 K. M. Tsoi, Q. Dai, B. A. Alman and W. C. W. Chan, *Acc. Chem. Res.*, 2013, **46**, 663.
7 L. J. Wang, G. Cao, T. Tu, H. O. Li, C. Zhou, X. J. Hao, Z. Su, G. C. Guo, H. W. Jiang and G. P. Guo, *App. Phys. Lett.*, 2010, **97**, 262113
8 M. Zhang, L. L. Bai, W. H. Shang, W. J. Xie, H. Ma, Y. Y. Fu, D. C. Fang, H. Sun, L. Z. Fan, M. Han, C. M. Liu and S. H. Yang, *J. Mater. Chem.*, 2012, **22**, 7461
9 S. Zhuo, M. Shao and S. T. Lee, *ACS Nano*, 2012, **6**, 1059
10 D. Pan, J. Zhang, Z. Li and M. Wu, *Adv. Mater.*, 2010, **22**, 735
11 S. J. Zhu, J. H. Zhang, X. Liu, B. Li, X. F. Wang, S. J. Tang, Q. N. Meng, Y. F. Li, C. S. Shi, R. Hu and B. Yang, *RSC Adv.*, 2012, **2**, 2717
12 N. Mohanty, D. Moore, Z. Xu, T. S. Sreeprasad, A. Nagaraja, A. A. Rodriguez and V. Berry, *Nat. Comm.*, 2012, **3**, 844
13 L. Tang, R. Ji, X. Cao, J. Lin, H. Jiang, X. Li, K. S. Teng, C. M. Luk, S. Zeng, J. Hao and S. P. Lau, *ACS Nano*, 2012, **6**, 5102
14 Z. P. Zhang, J. Zhang, N. Chen and L. T. Qu, *Energy Environ. Sci*., 2012, **5**, 8869.
15 J. H. Shen, Y. H. Zhu, C. Chen, X. L. Yang and C. Z. Li, *Chem. Commun.*, 2011, **47**, 2580.
16 F. Jiang, D. Q. Chen, R. M. Wang, G. Q. Zhang, S. M. Li, J. P. Zheng, N. Y. Huang, Y. Gu, C. R. Wang and C. Y. Shu, *Nanoscale*, 2013, **5**, 1137.
17 D. Y. Pan, J. C. Zhang, Z. Li and M. H. Wu, *Adv. Mater*. 2010, **22**, 734.
18 G. X. Zhao, L. Jiang, Y. D. He, J. X. Li, H. L. Dong, X. K. Wang and W. P. Hu, *Adv. Mater.*, 2011, **23**, 3959
19 A. D. L. Hoz, Á. D ńz-Oratiz, A. Moreno, *Chem. Soc. Rev.*, 2005, **34,** 164.
20 S. H. Park, S. M. Bak, K. H. Kim, J. P. Jegal, S. I. Lee, J. Lee, K. B. Kim, *J. Mater. Chem.*, 2011, **21** 680.
21 C. F. Wang, Y. J. Chen, K. L. Zhou and J. J. Wang, *Chem. Commun.*, 2013,**49**,3336.
22 D. W. Su, H. J. Ahn and G. X. Wang, *Chem. Commun.*, 2013, **49**, 3132.
23 Y. Q. Dong, J. W. Shao, C. Q. Chen, H. Li, R. X. Wang, Y. W. Chi, X. M. Lin, G. N. Chen,*Carbon*, 2012, **50**, 4740.
24 S. J. Zhu, J. H. Zhang, C. Y. Qiao, S. J. Tang, Y. F Li, W. J Yuan, B. Li, L. Tian, F. Liu, R. Hu, H. N. Gao, H. T. Wei, H. Zhang, H. C. Sun and B. Yang, *Chem. Commun.*, 2011, **47**, 6859.
25 G. Eda, Y. Y. Lin, C. Mattevi, H. Yamaguchi, H. A. Chen, S. Chen, C. W. Chen and M. Chhowalla, *Adv. Mater.*, 2010, **22** , 505.
26 Z. Liu, J. T. Robinson; X. M. Sun and H. J. Dai, *J. Am. Chem. Soc.*, 2008 , **130**, 10876.
27 Y. Li, Y. Zhao, H. H. Cheng, Y. Hu, G. Q. Shi, L. M. Dai and L. T. Qu, *J. Am. Chem. Soc*., 2012, **134**, 17.
28 R. Larciprete, A. Goldoni, A. Groso, S. Lizzit and G. Paolucci, *Surface science*, 2001, **136**, 482-485.
29 D. Pan, J. C. Zhang, Z. Li and M. H. Wu, *Adv. Mater.*, 2010, **22**,734.